Title

Distributed Fiber Optic Sensing to Identify Locations of Resistive Transitions in REBCO Conductors and Magnets

Journal

IEEE Transactions on Applied Superconductivity, 32(6)

ISSN

1051-8223

Authors

Luo, Linqing

Ferracin, Paolo

Stern, Jillian

et al.

Publication Date

2022

DOI

10.1109/tasc.2022.3159507

Distributed Fiber Optic Sensing to Identify Locations of Resistive Transitions in REBCO Conductors and Magnets

Linqing Luo, Paolo Ferracin, Jillian Stern, Danko van der Laan, Xiaorong Wang, Jeremy Weiss, Yuxin Wu

***Abstract*—High-temperature superconductors such as $REBa_2Cu_3O_{7-x}$ (REBCO, RE = rare earth) can generate strong magnetic fields that are promising for applications in particle accelerators and compact fusion reactors. Traditionally, voltage taps are installed in superconducting magnets to measure the voltage signals due to resistive transitions. The voltage-tap-based diagnostics is important for the development of magnet technology as it can help pinpoint the locations in the magnet windings that limit the magnet performance. The architecture of the multi-tape REBCO cable such as CORC® wires, however, makes it difficult to apply the voltage-tap-based diagnostics to identify the locations of resistive transitions. Distributed fiber optic sensing (DFOS) has the potential to address this issue. In this paper, we report the measurements of thermal strain along a CORC® wire based on optical frequency domain reflectometry with a maximum spatial resolution of 0.65 mm and a temporal resolution of 10 Hz. The optical fiber is co-wound with the CORC® wire that is epoxy impregnated. During the test, current was increased until a resistive transition occurred in the conductor. The spectrum shift of the reflected light along the fiber was recorded. The results suggested that with proper thermal isolation from the cryogen, DFOS can be used to identify the locations of resistive transitions in CORC® wires and magnets. The results will allow a better understanding of the causes of resistive transitions in REBCO conductors and magnets, which will help improve the REBCO magnet technology.**

***Index Terms*—High-temperature superconductor, REBCO cable, resistive transitions, distributed fiber optic sensing, defects localization**

I. Introduction

STRONG magnetic fields are used to confine the plasma for magnetic fusion research and accelerated particles in high-energy physics research. High-temperature superconductors (HTS) could allow for high magnetic fields and operation temperatures in fusion and high-energy physics research [1–3]. In the case of high-temperature superconducting $REBa_2Cu_3O_{7-x}$ (REBCO, RE = rare earth) tapes, high-field magnets for fusion and accelerator applications generally require multi-tape cables as magnet conductors [4][5].

One of the key needs for the development of high-field REBCO magnet technology is to identify and understand the locations of resistive transition, which can provide useful feedback on the development of HTS conductors and magnets [6]. Although voltage taps have been typically used to measure the resistive transition, it is not trivial to install or to install enough number of voltage-taps into the multi-tape and multi-layer REBCO cables to provide sufficient diagnostic signals. Other point sensors, such as thermometers and resistive strain gauges, face a similar issue for magnet diagnostics.

Fiber-optic based sensing has been studied as an alternative to voltage taps in HTS cables and magnets with the main goal of detecting quenches in HTS magnets by measuring the mechanical and thermal strain. The fiber Bragg grating (FBG) method has been tested for quench detection of an HTS fusion cable [7]. FBG is a pseudo-distributed sensing technology which can detect several sensing points in one optical fiber. Since the number of sensing points is limited and pre-defined, it can be difficult to localize the resistive transition regions that are usually unknown before the test.

Truly distributed fiber optic sensing (DFOS) was also studied, where the sensing fiber was embedded into no-insulation HTS coils to measure the temperature change with a Raman-scattering based detecting technology [8][9][10]. Brillouin-scattering based DFOS was also investigated to measure simultaneously the temperature and strain, demonstrating its potential for quench detection [11]. However, both Raman- and Brillouin-scattering based technologies have a relatively low spatial resolution (0.4-5m).

Rayleigh-scattering based DFOS was used to detect the temperature change with a high spatial resolution in the millimeter range [12]. The spectra shift of the Optical Frequency Domain Reflectometry (OFDR) was used to monitor a cryogenically

Manuscript receipt and acceptance dates will be inserted here. This work was supported by the Director, Office of Science, Office of Fusion Energy Sciences and the U.S. Magnet Development Program through Office of High Energy Physics of the US Department of Energy under Contract No. DEAC02-05CH11231, DE-SC0014009 and DE-SC0015775. This work was also supported by an LDRD program at LBNL.

(Corresponding author: Linqing Luo.)

L. Luo, P. Ferracin, J. Stern, X. Wang and Y. Wu are with Lawrence Berkeley National Laboratory, Berkeley, CA 94720 USA (email: linqingluo@lbl.gov).

J. Stern is also with Tufts University, 419 Boston Ave, Medford, MA 02155 USA

D. van der Laan and J. Weiss are with Advanced Conductor Technologies, LLC and the University of Colorado, Boulder, CO, 80301 USA.

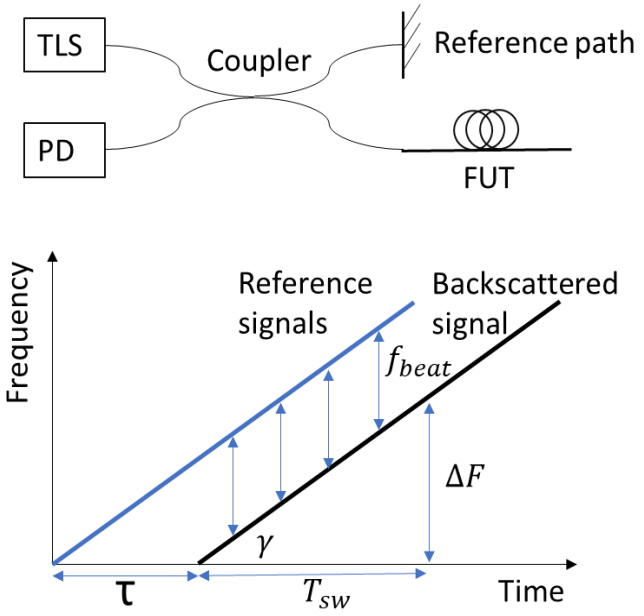

Fig. 1 The configuration of the Optical Frequency Domain Reflectometry (OFDR). TLS: Tunable Laser Source; PD: Photodetector; FUT: Fiber under test.

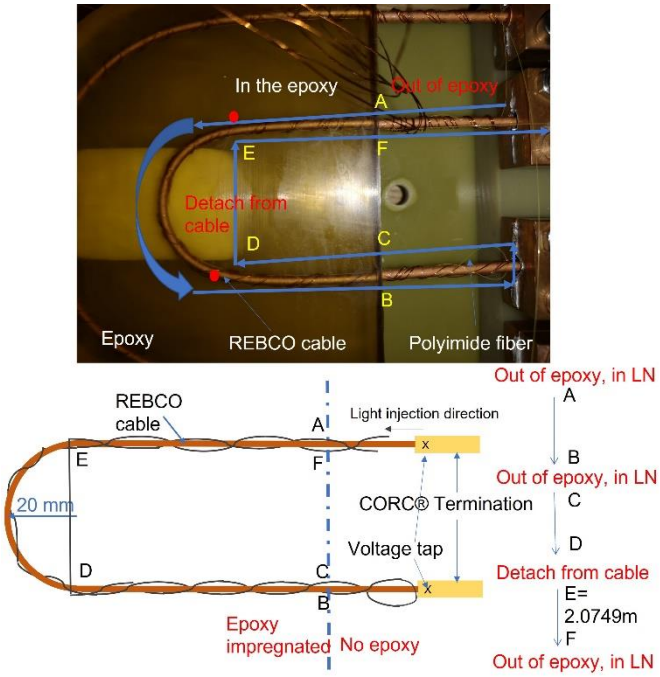

Fig. 2 The "U"-shaped CORC® wire and the co-wound optical fiber after the epoxy impregnation. "In LN" means the fiber directly in contact with liquid nitrogen. The location E is at about 2.0749 m in the fiber length.

cooled cable at 15 K [13]. The same technology was demonstrated to have a similar sensitivity at 77 K and room temperature in a subsequent study [14]. More recently, the OFDR technology was tested with an optical fiber embedded inside a REBCO CORC® cable for quench detection [15][16].

Although the fiber optic sensing shows a mixed performance for quench detection due to a stringent temporal resolution and high sensitivity to local heating [15-17], the distributed sensing capability of fiber optic remains attractive to address our need to identify the locations of initial flux-flow voltages in multi-tape REBCO cables and magnets.

In this paper, we studied the feasibility of OFDR technology in a DFOS sensor to localize the superconducting to normal transition in a CORC® wire [18][19]. With a spatial resolution of 0.65 mm and a temporal resolution of 10 Hz, we were able to identify the resistive transition at a curved section of the CORC® wire, and confirm the voltage rise across the CORC® wire was related to the local critical current (I_c) degradation due to bending. The experiments and results will allow us to apply the measurement technique in future magnets wound with multi-tape REBCO cables and understand the factors that limit the magnet performance.

II. Optical Frequency Domain Reflectometry

As one of the distributed fiber optic sensing methods, OFDR provides high spatial and temporal resolution by quantifying Rayleigh scattering that detects the change of the optical path length at each location on the fiber. As shown in Fig. 1, the measurement is based on the interference between two light reflection signals from the same tuning frequency laser source (TLS). The laser is connected to an optical coupler (OC) which splits the light beam into two paths. One launches into a reference arm which generates reflection with fixed travel time and phase. The other path, also called the sensing path, goes into the fiber under test (FUT). The scattered light interferes with the reflected reference light at the photodetector (PD) and the data is stored and analyzed by a computer. The laser is designed to have a tunable frequency with a fixed change rate γ. The signal from both paths beats at the PD, as described by [20][21]:

$$I(t) = |E_r(t) + E_s(t-\tau)|^2 = {E_0}^2\{1 + R + 2\sqrt{R}\cos[\omega_0 t + 2\pi\gamma\tau t - \pi\gamma\tau^2 + \varphi_0(t) - \varphi_0(t-\tau)]\}, \quad (1)$$

where E_0 is the input intensity at the path, ω_0 is the initial frequency, $\varphi_0(t)$ is the phase noise from the laser, f_s is the frequency span after time T_{sw}, which is the time interval between when light is injected into the fiber and the location that light is scattered back, R is the reflectivity of the FUT, τ is the time for light travelling from the scattering location to the photodetector before time t when the two lights interfere.

Here the $2\pi\gamma\tau$ is the beating frequency. The laser phase $\varphi_0(t) - \varphi_0(t-\tau)$ for a low phase noise laser can be negligible. The time delay τ is proportional to the speed of light and location, given as

$$\tau = \frac{L}{v} = \frac{Ln}{c}, \quad (2)$$

where c is the speed of light in vacuum, n is the refractive index, and L is the location of scattering.

The interference frequency of the detected signal is proportional to the location on the fiber. By analyzing different frequency components of the detected signal from PD, signals at each location on the FUT can be interrogated. When strain or temperature changes on the FUT, it will introduce a slowly varying envelop at a frequency at the location. The variation in the

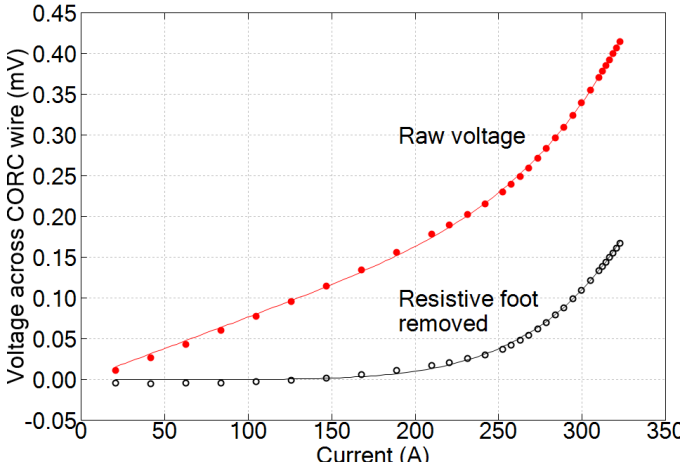

Fig. 3 The measured voltage across the CORC® wire's termination at 77 K, self-field. Red solid circles: raw voltage. Black open circles: voltage with the contribution from the termination removed. Solid lines: exponential fit.

envelop can be obtained by correlating both readings. A reference reading is recorded first when no strain and uniform temperature is applied to the FUT. By correlating the readings to the reference, one can obtain a frequency shift which linearly indicates the change of strain and temperature on the FUT [16][20][21]:

$$\Delta f = k_T \Delta T + k_\varepsilon \Delta \varepsilon \quad (2)$$

where Δf is the spectral frequency shift, k_T is the linear coefficient for temperature, ΔT is the temperature change, $\Delta \varepsilon$ is the strain change, and k_ε is the linear coefficient for strain.

III. Experiment Set-up and Measurement Protocol

The measurement was performed as part of an epoxy impregnation test of a CORC® wire. The CORC® wire used in the experiments is 0.178 m long. The details on the CORC® wire used here can be seen in [18][19][22]. The wire contains six REBCO tapes commercially available from SuperPower Inc. The wire was first bent with a 2 cm radius and an optic fiber was co-wound around the wire afterwards. Then the wire and fiber were impregnated with an epoxy (NHMFL Mix 61) and cured for 16 hours at 60 ˚C and 24 hours at 100˚C [22].

Fig. 2 shows the CORC® wire and fiber optic sensor after impregnation. The optical fiber was wrapped around the CORC® wire from the top right. The labels "A" through "F" in Fig. 2 illustrate the fiber locations on the CORC® wire. The fiber entered the epoxy at point A, following the conductor until point B, and then exited the epoxy. The fiber entered the epoxy again at point C and followed the CORC® wire until point D. The fiber was routed from point D directly to point E, bypassing the CORC® wire, and then followed CORC® wire again and exited the epoxy at point F. Point E is at about 2.0749 m in the fiber length. The optical fiber was wrapped with tension and behaved like a spring wrapping tightly around the CORC® wire as the fiber tended to reduce its axial strain. The friction between the optical fiber and CORC® wire also helped hold the optical fiber around the CORC® wire. As a result, the optical fiber was in surface contact after co-wounding. After the epoxy impregnation, the fiber was completely captured inside the

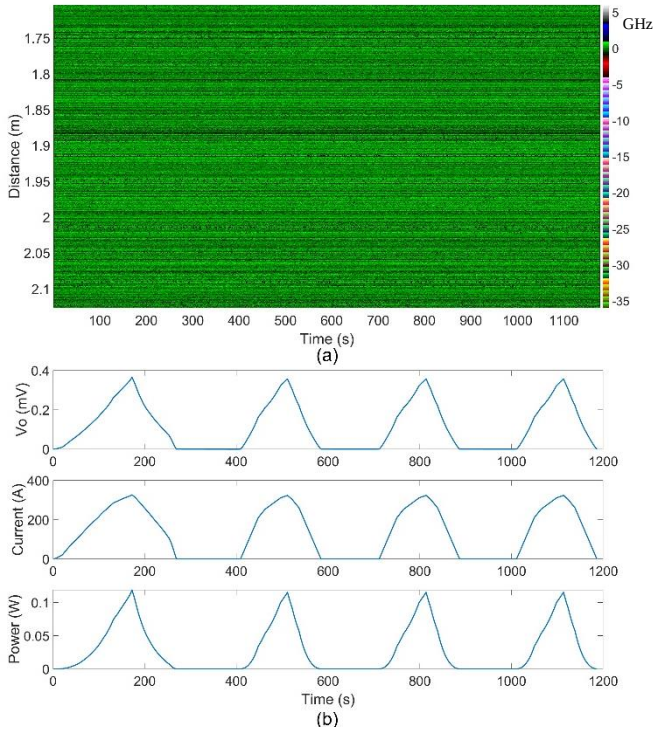

Fig. 4 The result before the epoxy impregnation. (a) The response of the OFDR sensor without impregnation. Vertical axis is the actual length of the optical fiber. (b) The plot of voltage, current input, and power on the tested sample, the current maximized at 325 A, 317.6 A, 322.9 A, and 322.9 A respectively in each ramp.

epoxy resin and was not in direct contact with the cryogen during subsequent measurements. The optical fiber section between A and B was in direct contact with CORC® wire while the optical fiber sections between C and D, E and F need to cross over the optical fiber section between A and B. Therefore, the optical fiber sections between C and D, E and F can be less sensitive than the optical fiber section between A and B at the crossover locations.

A commercial OFDR system, Luna ODiSi, was used to measure the temperature change in the CORC® wire. The system has a spatial resolution of 0.65 mm, and an accuracy of 1 micro-strain or 0.1 ˚C temperature change. The optical fiber is a low bend loss, 9/125 single mode fiber with a 12.5 µm thick polyimide coating. The linear coefficient k_T for temperature is about -0.638 ℃/GHz. Since the CORC® wire and fiber were encapsulated in epoxy and no mechanical force was applied to the sample, the strain was ignored in the measurements.

The I_c of the CORC® wire was measured, before and after impregnation, in liquid nitrogen at 77 K and self-field. The fiber response was measured during both 77 K tests, together with the voltage across the CORC® wire and the transport current generated by a current source controlled manually during the tests.

The measurements included four parts. Part A was the measurement of the critical current I_c of the CORC® wire before and after epoxy impregnation. With the measured critical current, we determined the maximum current for the following measurements.

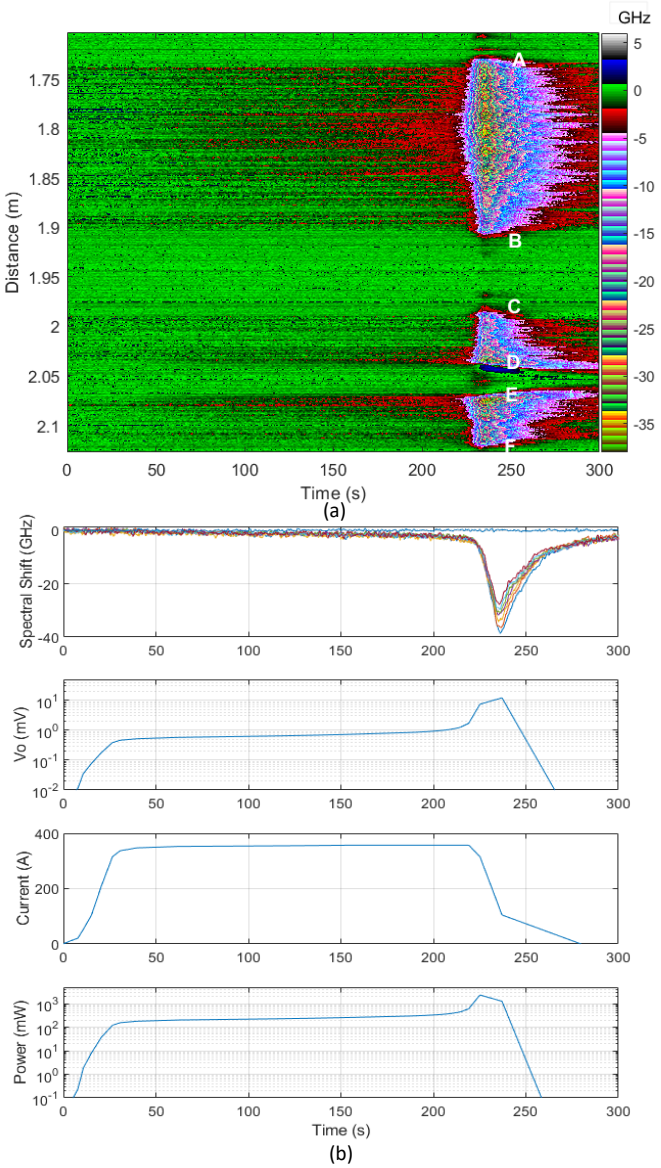

Fig. 5 The result of Test 1 after epoxy impregnation. (a) The response received by the OFDR sensor. Vertical axis is the actual length of the optical fiber. (b) Evolution of 1) spectral shift at the locations close to point E (7 points between 2.0749 m to 2.0788 m), 2) voltage V across the CORC® wire, 3) current I (maximized at about 356.8 A), and 4) total power generated as determined by $V I$.

From Part B to D, we measured the optical fiber sensor response when the injected current was slightly higher than I_c. The fiber optic sensor recorded the frequency shift along the optical fiber with 0.65 mm spatial interval and 10 Hz time interval. During each measurement, the current was injected into the CORC® wire and the frequency shift at each location were recorded and analyzed to check whether the temperature increase can be observed from the frequency shift data when the current was higher than the critical current.

In Part B, four current ramps were performed with a peak power of about 0.12 W generated in the CORC® wire. We measured the frequency shift on the optical fiber when the CORC® wire and optical fiber before the impregnation.

In Parts C and D, we measured the frequency shift of the optical fiber after impregnation. Part C was performed with a fast ramp that the current went beyond the critical current (as Test 1). The current first rapidly increased to 336 A, then the current gradually increased to 356.8 A in the next 190 s. Then the current was reduced to 104.7 A and kept reducing to 0 A.

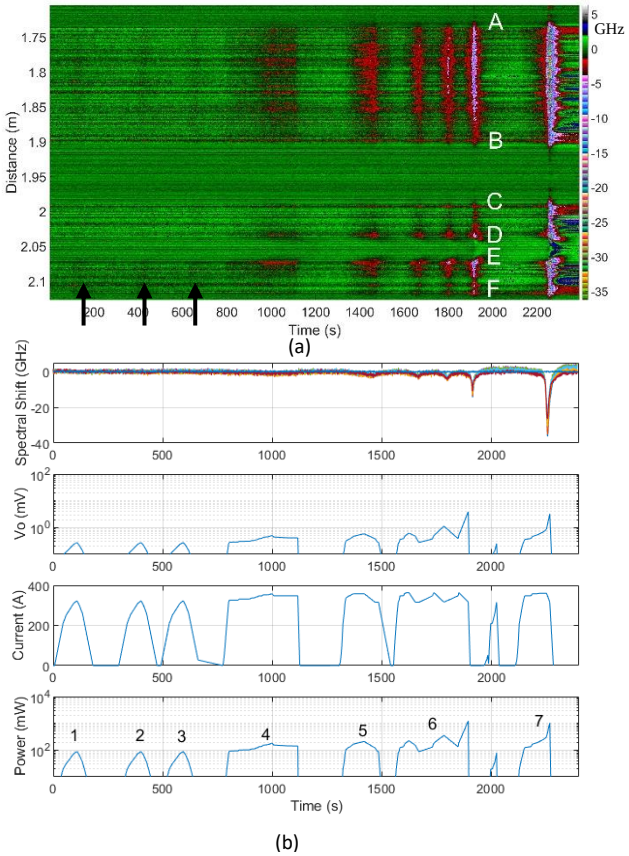

Fig. 6 The result of Test 2 after the epoxy impregnation. (a) The response received by OFDR sensor. Vertical axis is the actual length of the optical fiber. (b) Evolution of 1) spectral shift at the locations close to point E (7 points between 2.0749 m to 2.0788 m); 2) voltage across the CORC® wire; 3) current I (each ramp maximized at 320.7 A, 316.5 A, 322.8 A, 347.3 A, 352.5 A, 358 A, and 360.1 A respectively) and 4) the total power generated.

In Part D, we applied current ramps with different maximum currents and investigated the response of the optical fiber (as Test 2). The first three ramps were the current cycles between 0 and 322 A with a peak power of about 0.13 W in each ramp. Then at around 1000 s, for Ramp 4, the current increased to 347.3 A. The peak current was 352.5 A for Ramp 5 and 358 A for Ramp 6. Ramp 6 included three sub-ramps around the maximum current value. Finally, the current increased to 360.1 A in the last ramp and decreased to zero rapidly.

Same reference for the optical fiber sensor OFDR reading were used in Part C and D and the time interval between the Part C and D was about 30 minutes.

IV. Result and Discussion

A. *Voltage as a function of current of the CORC® wire*

Fig. 3 shows the voltage across the CORC® wire measured at 77 K, self-field, in one of the measurements after the epoxy impregnation. The I_c of the wire, determined at a voltage

criterion of 20 μV, is 224 A [22]. The raw voltage included a linear voltage component (resistive foot) that is due to the termination joint resistance. The CORC® wire had a higher I_c of 265 A before impregnation, and the *V(I)* curve contained a similar resisitive voltage component as shown in Fig. 3.

B. 77 K measurement before the epoxy impregnation

Fig. 4 shows the measurement results from the co-wound optic fiber at 77 K before the epoxy impregnation. One sees that the optic fiber was not sensitive enough to measure any temperature rise due to the resistive heating from the sample, despite a repetitive peak power of 0.12 W generated in the CORC® wire. The optic fiber essentially measured a constant temperature of liquid nitrogen during the test. The lack of response in the optic fiber can be attributed to the direct contact between the CORC® wire and cryogen and between the optical fiber and cryogen. The heat generated in the wire was dissipated through heat transfer with the surrounding cryogen, leading to negligible temperature rise in the CORC® wire. We were not able to check the contact condition between the fiber and CORC® wire after the cooldown to 77 K. Therefore, one may argue that the lack of response in the fiber can also be due to the potential loose contact between the fiber and CORC® wire after the cooldown. On the other hand, a visual inspection of the CORC® wire and fiber at room temperature after the test showed that the fiber was in the same contact condition as before the cooldown.

C. 77 K measurement after the epoxy impregnation, Test 1

Fig. 5 shows the measurement results after the impregnation. The frequency shift was referenced to the readings before the current injection. The green color shows the noise level when no temperature change was measured by the fiber. The voltage across the CORC® wire increased to 0.4 mV when the current reached 336 A. The voltage kept rising and eventually reached about 12 mV before the current was reduced to 104.7 A. The heating power in the CORC® wire peaked at 2.34 W at about 225 s.

The associated temperature rise was successfully measured by the fiber, as shown in Fig. 5a where points A-F correspond to the fiber locations in Fig. 2. The heating in the CORC® wire sections AB, CD and EF was identified. The fiber did not measure any temperature change between points D and E where the fiber bypassed the CORC® wire (lose contact with the CORC® wire) and between points B and C where the fiber was in contact with the cryogen, consistent with the test results before impregnation.

Fig. 5a also showed that the heating was first sensed at the center of the "U"- shaped bend region of the CORC® wire, as indicated by the spectral shift at around 100 s in the central region between points A and B and at point E. Although the change of the spectral shift was insignificant (less than 3 GHz, green or red color in Fig. 5a) until around 220 s when the voltage runaway occurred, clearly insufficient for quench detection, the optic fiber was able to identify the heating region in the CORC® wire where the I_c was likely degraded due to bending. This information was otherwise unavailable from the voltage signal across the CORC® wire and is important to understand the causes of the observed voltage rise.

D. 77 K measurement after the epoxy impregnation, Test 2

The experiment result for Test 2 after the impregnation is shown in Fig. 6. The green color shows the noise level when no temperature change was measured. At about 180 s, 400 s, and 650 s, the spectral shifted slightly in the fiber signal as indicated by the arrows in Fig. 6a. These three ramps were part of the I_c measurements where the current cycled between 0 and 322 A with a maximum power of about 0.13 W in each ramp. The appearance of the slightly darker color in Fig. 6a indicated that the sensitivity of the fiber was barely enough to sense the heat generated when the current was around the I_c.

At about 1000 s, the fiber responded to the local temperature rise again with a more pronounced spectral shift due to stronger heating. The spectral shift occurred again in the central region between point A and B and close to point E. As the heating continued, the normal zone expanded from the bent region into sections CD and EF, the straight part of the CORC® wires, as indicated by the spectral shift at 1800 and 1900 s. During the last ramp that started around 2050 s, the whole wire was heated as indicated by the spectral shift covering the entire length of the CORC® wire inside the epoxy.

Comparing the spectral shift of the last four current ramps, especially the 4th and 5th ramps, one sees that although the power generated during the 5th ramp was lower than that of the 4th ramp, the 5th ramp led to a stronger spectral shift. This indicated that as the current ramped more frequently, the temperature of the CORC® wire may not recover to 77 K after each current ramp, an effect that can be enhanced by epoxy impregnation.

Comparing the results in the tests before and after impregnation, one sees that the epoxy can help improve the sensitivity of DFOS by isolating the cryogen from the CORC® wire and sensing fibers. The results from both tests after epoxy impregnation suggested that the optic fiber co-wound around the CORC® wire can be sensitive to a total heating power of 0.2 W in the experimental condition reported here. The power corresponds to 5 kA and 40 μV voltage rise, a level that was observed in recent REBCO magnet tests [23][24]. Therefore, a similar measurement DFOS setup can potentially identify the transitioning region in magnets. In addition, the optical power loss was not analyzed either after the optical fiber was co-wound to the CORC® wire or after impregnation. As the optical power loss after the attachment can affect the measurement resolution, the measurement sensitivity can be improved by testing the optical power loss with different attachment methods in our future research.

V. Conclusion and future plans

This paper investigated optical frequency domain reflectometry (OFDR) based distributed fiber optic sensing system to identify the locations of the resistive transition in a CORC® wire. The optical fiber was co-wound with the sample, followed by epoxy impregnation. During the test, the heating in the bent region of the CORC® wire was successfully localized when the total heating power was about 0.13 – 0.21 W. The results show that OFDR based fiber optic sensing can be sensitive to the heating at a power level of 0.2 W when the CORC® wire and fiber sensor are impregnated and isolated from cryogen.

The measurement technique needs to be tested in magnets at 4.2 K where the sensitivity of fiber can be lower than 77 K. Methods will also be investigated to improve the fiber sensitivity and survival rate in cryogenic environments. Alternative methods to attach the fiber to HTS conductors will also be studied to ensure the constant contact at various testing temperatures.

Acknowledgment

We thank T. Bogdanof, M. Krutulis, and J. Swanson for sample preparation and help during the test.

References

[1] Z. S. Hartwig, C. B. Haakonsen, R. T. Mumgaard, and L. Bromberg, "An initial study of demountable high-temperature superconducting toroidal field magnets for the Vulcan tokamak conceptual design," *Fusion Eng. Des.*, vol. 87, no. 3, pp. 201–214, 2012, doi: 10.1016/j.fusengdes.2011.10.002.

[2] B. N. Sorbom *et al.*, "ARC: A compact, high-field, fusion nuclear science facility and demonstration power plant with demountable magnets," *Fusion Eng. Des.*, vol. 100, pp. 378–405, 2015, doi: 10.1016/j.fusengdes.2015.07.008.

[3] S. A. Gourlay, "Superconducting accelerator magnet technology in the 21st century: A new paradigm on the horizon?," *Nucl. Instruments Methods Phys. Res. Sect. A Accel. Spectrometers, Detect. Assoc. Equip.*, vol. 893, pp. 124–137, 2018, doi: 10.1016/j.nima.2018.03.004.

[4] D. Uglietti, "A review of commercial high temperature superconducting materials for large magnets: From wires and tapes to cables and conductors," *Supercond. Sci. Technol.*, vol. 32, no. 5, 2019, doi: 10.1088/1361-6668/ab06a2.

[5] Z. S. Hartwig *et al.*, "VIPER: An industrially scalable high-current high-temperature superconductor cable," *Supercond. Sci. Technol.*, vol. 33, no. 11, 2020, doi: 10.1088/1361-6668/abb8c0.

[6] X. Wang, S. A. Gourlay, and S. O. Prestemon, "Dipole Magnets Above 20 Tesla: Research Needs for a Path via High-Temperature Superconducting REBCO Conductors," *Instruments*, vol. 3, no. 4, p. 62, Nov. 2019, doi: 10.3390/instruments3040062.

[7] E. E. Salazar *et al.*, "Fiber optic quench detection for large-scale HTS magnets demonstrated on VIPER cable during high-fidelity testing at the SULTAN facility," *Supercond. Sci. Technol.*, vol. 34, no. 3, 2021, doi: 10.1088/1361-6668/abdba8.

[8] J. Jiang *et al.*, "Bend limitation of a polyimide-coated optical fiber at cryogenic temperature of 77 K," *IEEE Trans. Appl. Supercond.*, vol. 29, no. 2, Mar. 2019, doi: 10.1109/TASC.2018.2883734.

[9] J. Jiang *et al.*, "Experimental Study on Quench Detection of a No-Insulation HTS Coil Based on Raman-Scattering Technology in Optical Fiber," *IEEE Trans. Appl. Supercond.*, vol. 28, no. 3, pp. 1–5, 2018, doi: 10.1109/TASC.2018.2802487.

[10] J. Jiang *et al.*, "Thermal Stability Study of a Solder-Impregnated No-Insulation HTS Coil Via a Raman-Based Distributed Optical Fiber Sensor System," *IEEE Trans. Appl. Supercond.*, vol. 29, no. 2, Mar. 2019, doi: 10.1109/TASC.2018.2890384.

[11] S. Mahar *et al.*, "Real-time simultaneous temperature and strain measurements at cryogenic temperatures in an optical fiber," *Remote Sens. Syst. Eng.*, vol. 7087, pp. 70870I-70870I–12, 2008, doi: 10.1117/12.791913.

[12] F. Scurti, S. Ishmael, G. Flanagan, and J. Schwartz, "Quench detection for high temperature superconductor magnets: A novel technique based on Rayleigh-backscattering interrogated optical fibers," *Supercond. Sci. Technol.*, vol. 29, no. 3, p. 03LT01, 2016, doi: 10.1088/0953-2048/29/3/03LT01.

[13] C. D. Boyd, E. E. Horrell, E. M. Lally, and B. D. Dickerson, "Verifying cryogenic cooling of superconducting cables using optical fiber," in *2012 Future of Instrumentation International Workshop (FIIW) Proceedings*, 2012, pp. 1–4, doi: 10.1109/FIIW.2012.6378335.

[14] Y. Du *et al.*, "Cryogenic temperature measurement using Rayleigh backscattering spectra shift by OFDR," *IEEE Photonics Technol. Lett.*, vol. 26, no. 11, pp. 1150–1153, Jun. 2014, doi: 10.1109/LPT.2014.2317702.

[15] D. C. van der Laan, J. D. Weiss, F. Scurti, and J. Schwartz, "CORC® wires containing integrated optical fibers for temperature and strain monitoring and voltage wires for reliable quench detection," *Supercond. Sci. Technol.*, vol. 33, no. 8, Aug. 2020, doi: 10.1088/1361-6668/ab9ad1.

[16] F. Scurti, J. D. Weiss, D. C. van der Laan, and J. Schwartz, "SMART conductor on round core (CORC®) wire via integrated optical fibers," *Supercond. Sci. Technol.*, vol. 34, no. 3, 2021, doi: 10.1088/1361-6668/abdc7f.

[17] B. Chen *et al.*, "Quench Detection of Bi2223/Ag Insulated Double-Pancake Coil Using Distributed Optic Fiber Sensor," *IEEE Trans. Appl. Supercond.*, vol. 30, no. 3, Apr. 2020, doi: 10.1109/TASC.2019.2929479.

[18] J. D. Weiss *et al.*, "Introduction of the next generation of CORC® wires with engineering current density exceeding 650 A mm-2 at 12 T based on SuperPower's ReBCO tapes containing substrates of 25 µm thickness," *Supercond. Sci. Technol.*, vol. 33, no. 4, 2020, doi: 10.1088/1361-6668/ab72c6.

[19] D. C. van der Laan, J. D. Weiss, and D. M. McRae, "Status of CORC® cables and wires for use in high-field magnets and power systems a decade after their introduction," *Supercond. Sci. Technol.*, vol. 32, no. 3, 2019, doi: 10.1088/1361-6668/aafc82.

[20] Y. Yu *et al.*, "Distributed thermal monitoring of lithium ion batteries with optical fibre sensors," *J. Energy Storage*, vol. 39, Jul. 2021, doi: 10.1016/j.est.2021.102560.

[21] P. Lu *et al.*, "Distributed optical fiber sensing: Review and perspective," *Applied Physics Reviews*, vol. 6, no. 4. American Institute of Physics Inc., 01-Dec-2019, doi: 10.1063/1.5113955.

[22] J. Stern, T. Bogdanof, J. Swanson, D. van der Laan, X. Wang, and J. Weiss, "Developing a Vacuum Pressure Impregnation Procedure for CORC® Wires," in *27th International Conference on Magnet Technology*, 2021, p. FRI-OR6-603-02.

[23] D. C. van der Laan *et al.*, "A CORC® cable insert solenoid: The first high-temperature superconducting insert magnet tested at currents exceeding 4 kA in 14 T background magnetic field," *Supercond. Sci. Technol.*, vol. 33, no. 5, 2020, doi: 10.1088/1361-6668/ab7fbe.

[24] X. Wang *et al.*, "Development and performance of a 2.9 Tesla dipole magnet using high-temperature superconducting CORC®wires," *Supercond. Sci. Technol.*, vol. 34, no. 1, 2021, doi: 10.1088/1361-6668/abc2a5.